

# Seismic Performance of Dual Systems with BRBs under Mainshock-Aftershock Sequences

Francesco Morfuni

*PhD Student, Dept. of Civil, Environmental and Geomatic Engineering, University College of London, London, UK*

Fabio Freddi

*Lecturer, Dept. of Civil, Environmental and Geomatic Engineering, University College of London, London, UK*

Carmine Galasso

*Associate Professor, Dept. of Civil, Environmental and Geomatic Engineering, University College of London, London, UK*

**ABSTRACT:** Buckling-restrained braces (BRBs) are employed in new constructions and in the retrofiting of existing frames. They provide additional strength and stiffness to buildings, together with high and stable energy dissipation capacity. BRBs can fail due to excessive maximum and/or cumulative ductility demands. In addition, the use of BRBs can result in large residual drifts in the structure due to their low post-elastic hardening. Moreover, in seismic-prone regions, structures are usually subjected to mainshock-aftershocks (MS-AS) earthquake sequences, often leaving no time for repair or retrofit between events. Ductility demand accumulation and/or residual drifts induced by the MS can affect the structural performance during the following AS. The present study addressed the abovementioned issues by first investigating an optimal design procedure for steel dual systems in which conventional BRB frames are combined with moment-resisting frames. The latter are designed to behave elastically to enhance the self-centering capability of the structure and limit soft-story mechanisms. The design procedure is first presented and applied to a case-study building. The seismic performance of the latter is assessed by means of sequential Cloud Analysis. Both real and artificial MS-AS sequences are used to derive system fragility curves. Results show that the BRB's capacity can be potentially affected by multiple earthquakes, which cause accumulation of plastic strains within the devices. However, the preliminary results show that when accounting for real MS-AS sequences, ASs do not significantly increase the cumulative ductility demands in BRBs.

## 1. INTRODUCTION

Buckling-restrained braces (BRBs) have emerged as effective passive control systems to improve the seismic performance of newly designed and existing buildings. In BRBs, a sleeve provides buckling resistance to an unbonded core that resists the axial stress. As buckling is prevented, BRBs behave in a similar way in tension and in compression allowing for the development of stable hysteretic cycles, providing significant energy dissipation capacity (*e.g.*, Zona & Dall'Asta 2012a).

BRBs failure can be related to excessive maximum or cumulative ductility demand (*e.g.*, Fahnestock et al. 2003). Moreover, BRBs are characterized by low post-elastic hardening that can result in large residual deformations, and hence, can lead to moderate-to-high residual drifts in the structure (Sabelli et al. 2003).

Several studies investigated BRBs behavior (*e.g.*, Di Sarno & Manfredi 2010, Freddi et al. 2013, Tubaldi et al. 2017) on newly designed structures and for the retrofit of existing ones; however, most of those studies evaluate the

seismic performance of the structure by considering the effect of a single earthquake only (*i.e.*, the mainshock). However, in seismically active regions, structures are typically subjected to mainshock-aftershock (MS-AS) sequences, often leaving no time for repair or retrofit between events. Hence, the seismic performance of structures equipped with BRBs should be evaluated considering MS-AS sequences (*e.g.*, Raghunandan et al. 2015, Jalayer & Ebrahimiyan 2017) in order to properly account for their cumulative ductility demand.

To address the drawbacks of conventional BRB frames (BRBFs), several studies investigated the feasibility of steel dual systems, where a back-up moment resisting frame (MRF) is combined with a BRBF (*e.g.*, Kiggins & Uang 2006, Maley et al. 2010, Ariyaratana & Fahnestock 2011, Terán-Gilmore et al. 2015, Baiguera et al. 2016). In dual systems, the MRF, providing an additional load path, can be designed to behave elastically in order to improve the self-centering capability of the system. In this way, the MRF contributes also to the redistribution of the lateral forces along the height of the building, reducing the potential formation of soft-story mechanisms. Furthermore, the energy dissipation is provided by the BRBs only that, acting as structural fuses, can be easily replaced when damaged.

The present study investigates a design procedure for dual systems comprising MRFs and BRBFs. A case-study building is designed, modeled in OpenSees (McKenna et al. 2006), and assessed by means of Cloud Analysis accounting for MS-AS sequences. Real and synthetic MS-AS sequences are selected as input for non-linear time history analyses. The results show that the use of dual systems including MRFs and BRBFs adequately designed allows to achieve a resilient structure able to sustain MS-AS sequences, that concentrates the damage on easy to replace fuses and that limits the residual drifts.

## 2. DUAL SYSTEM DESIGN

Figure 1 shows the geometry of an 8-story steel building located in Norcia, Italy, used as a case-

study building. In each direction, two MRFs are coupled with two BRBFs by means of a rigid diaphragm at each floor. The steel braces are composed by dissipative BRB devices and elastic steel braces arranged in series, allowing for the independent calibration of their yielding force ( $F_y$ ) and stiffness ( $K$ ) (Dall'Asta et al. 2009). Given the symmetry of the geometry and loading condition, the design is limited to a single dual system. A summary of the design details for the MRF and for the braces of the BRBF is given in Table 1. Beams and columns of the BRBF are respectively W18×55 and W14×90 for the first four floors, while W18×50 and W14×53 are chosen for the four uppermost ones.

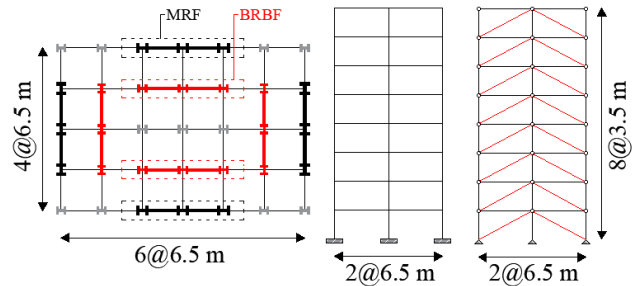


Figure 1: Case-study building: plan view (left) and elevation view of the MRF and BRBF (right).

Table 1: W-beam profiles for the MRF and yielding force and stiffness of braces of the BRBF.

Floor	MRF			BRBF	
	Beam	Ext Col	Int Col	$F_y$ [kN]	$K$ [MN/m]
1	18×71	14×132	14×132	547.2	172.6
2	18×71	14×82	14×120	537.6	106.2
3	18×65	14×74	14×120	511.8	98.9
4	18×60	14×68	14×120	468.6	94.6
5	18×50	14×61	14×99	407.8	84.7
6	18×40	14×53	14×82	329.1	73.7
7	18×35	14×48	14×82	232.7	69.2
8	18×35	14×38	14×61	121.4	33.9

The design of the dual system is fully governed by three variables, such as the ductility demands respectively for the MRF ( $\mu_{MRF}$ ) and for the BRBF ( $\mu_{BRB}$ ) and the strength proportion coefficient ( $\alpha$ ). The  $\alpha$ -coefficient defines the ratio

between the seismic base shears carried by the BRBF ( $V_{BRB}$ ) and MRF ( $V_{MRF}$ ) respectively. For newly-designed structures,  $\alpha$  is selected depending on the performance requirements that the designer attributes to the two components of the dual system. According to SEI/ASCE 7-10 (ASCE 2010), the MRF is required to resist at least 25% of the total base shear and hence  $\alpha$  should not be greater than 3. In this study  $\alpha$  is assumed equal to 1. Moreover, if the elastic behavior of the MRF is enforced,  $\mu_{MRF}$  must be set equal to 1 and, consequently, the design maximum inter-story drift ( $\theta_d$ ) should not exceed the yielding limit (Garcia et al. 2010). Lower values of  $\theta_d$  might be selected, where appropriate, to limit damage in the non-structural elements (e.g., Eurocode 8; CEN 2004). Once the  $\theta_d$  value is defined, the design deformed shape of the system is derived based on the displacement-based design (DBD) procedure (Priestley et al. 2007). Finally, the BRBF can be assumed as an equivalent elastic-perfectly plastic component with a given ductility  $\mu_{BRB}$ . The selection of all the variables is summarized in Figure 2, which illustrates, in the acceleration-displacement (AD) plane, the elastic behavior and the elasto-plastic behavior respectively for the equivalent single degree of freedom (SDOF) systems (Fajfar 2000) of the MRF and the BRBF. The behavior of the dual system with the components working in parallel and the equivalent bilinear elasto-perfectly plastic system are also reported.

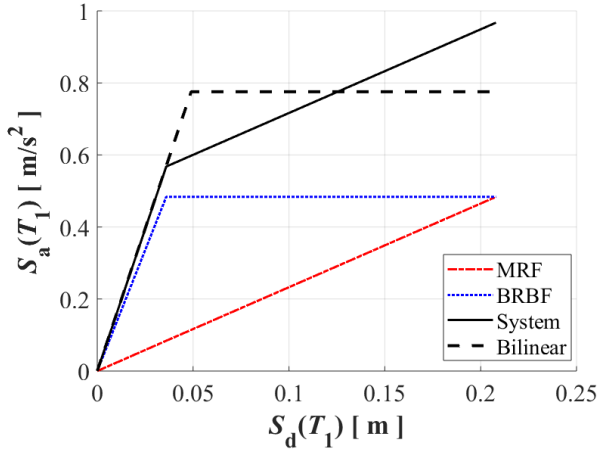


Figure 2: Design components and system capacity curves.

The design base shear of the dual system and the BRB ductility can be selected iteratively so that the bi-linearized capacity of the equivalent SDOF system matches the seismic inelastic demand expected at the site, based on the N2 method (Fajfar 2000), as shown in Figure 3. The reader might note that the corner period ( $T_D$ ) of the AD demand spectrum has been shifted from 2 (Eurocode 8) to 8 seconds, as recommended by Faccioli et al. (2004) if the displacement spectrum governs the design.

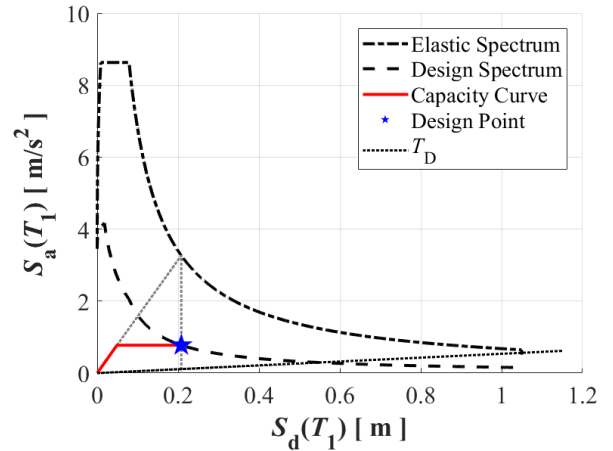


Figure 3: Performance point of the equivalent SDOF.

Once the key variables are known, it is then possible to design the primary elements of the MRF and the BRBF. Equivalent lateral forces acting on the MRF are determined following the DBD approach, also accounting for the presence of higher-modes effects. Internal forces on beams and columns are then computed based on the equilibrium approach (Priestley et al. 2007). In line with other similar works (Maley et al. 2010), beams are sized according to their seismic flexural demand only, neglecting the contribution of gravity loads. The latter are sustained by orthogonal frames, due to the presence of a one-way slab which runs parallel to the direction of analysis. However, it is noteworthy that, given the elastic behavior of the MRF, it is not possible to rely on the full plastic capacity of the section. Hence, the flexural resistance is computed based on the elastic modulus of the section ( $W_{el}$ ) and not on the plastic one ( $W_{pl}$ ). The same consideration also applies to vertical elements, whose design

also accounts for the presence of the axial load and for the buckling checks (according to Eurocode 8).

BRBs are then designed following the methodology proposed by Dall'Asta et al. (2009) that has been extended in order to account for the axial deformability of columns (Maley et al. 2010, Ragni et al. 2011). Finally, beams and columns of the BRBF, assumed pinned at the joints, are designed in overstrength, following the capacity design provisions to ensure that damage is concentrated within BRBs only.

### 3. NONLINEAR MODELS

The prototype dual system is modeled in OpenSees. Columns of the MRF are modeled using non-linear force-based beam-column elements. A bilinear elastoplastic material (*Steel01* with yielding strength equal to 355 MPa and 0.2% strain hardening) is assigned to the section fibers. Beams are modeled as elastic elements with lumped plasticity modeled by zero length rotational springs at their ends. Such springs are characterized by the degrading modified Ibarra-Medina-Krawinkler hysteretic bilinear model (Ibarra et al. 2005, Lignos & Krawinkler 2011). Stiffness matrices of the elastic elements between plastic hinges are modified through the 'n' modification factor (Zareian & Medina 2010) allowing for the use of initial stiffness proportional Rayleigh damping, with 3% of the critical damping assigned to the 1<sup>st</sup> and 2<sup>nd</sup> modes. MRF panel zones are modeled using the Scissors approach (Castro et al. 2005) to account for the deformability of columns' webs and flanges.

Beams and columns of the BRBF are modeled by elastic beam-column elements with negligible inertia to reproduce pinned connections. BRBs are modelled with truss elements having elastic links to represent the elastic component of the brace. The steelBRB material (Gu et al. 2014) is used to model the BRB device (Figure 4) using the material's parameters identified by Zona & Dall'Asta (2012a).

To account for P- $\Delta$  effects, the gravity columns are modeled with an equivalent

continuous lean-on column, pinned at its base, as done in Freddi et al. (2017). Finally, diaphragm action is accounted by means of rigid truss elements connecting the nodes of the lean-on column to the ones of the beams of the MRF and of the BRBF.

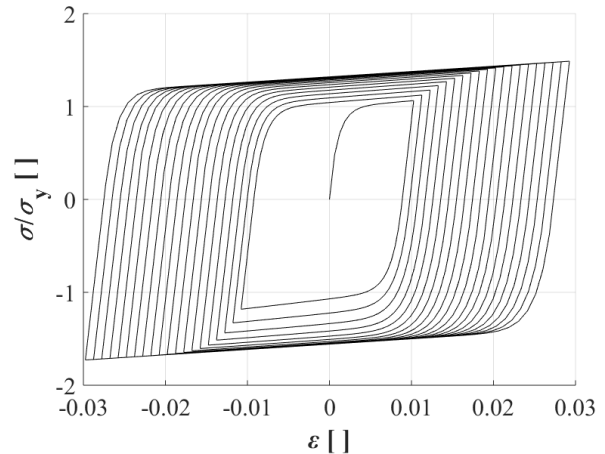


Figure 4: Cyclic response of the steelBRB material under sinusoidal history with increasing amplitude.

The design procedure is validated by the comparison of the non-linear static analysis performed in OpenSees and the design objective of Figure 2. The comparison, reported in Figure 5, shows minor differences ascribed to the initial design assumptions. In particular, the design neglects the strain hardening of BRBs as well as the redistribution along the height of lateral forces operated by the lean-on column.

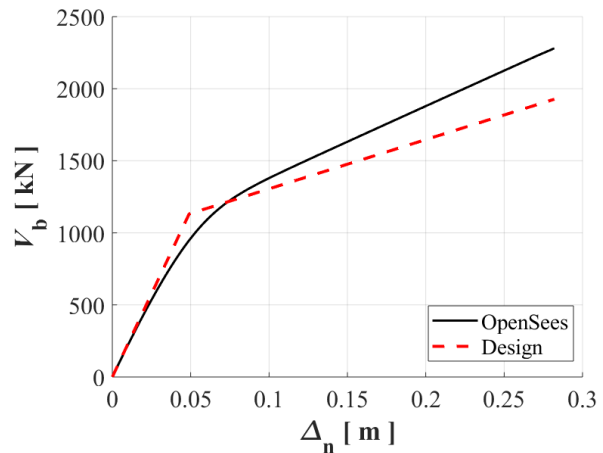


Figure 5: Comparison of Design and OpenSees Pushover curves.



#### 4. RECORDS SELECTION

A suite of 199 MS-AS ground motion sequences is extracted from a set of records originally developed by Goda & Taylor (2012). Events with MS spectral acceleration at the fundamental period ( $S_{a,MS}(T_1)$ ; with  $T_1$  equal to 1.6s) lower than 0.035g are arbitrarily disregarded in this study since for these intensities the structure behaves elastically. In a similar way, records with a ratio of  $S_{a,AS}(T_1)/S_{a,MS}(T_1)$  (where  $S_{a,AS}(T_1)$  stands for the AS spectral acceleration at  $T_1$ ) lower than 0.3 are neglected, providing the AS is not likely to induce additional damage. Combination of the spectral accelerations for the resulting 199 MS-AS sequences is plotted in Figure 6, together with the abovementioned selection criteria.

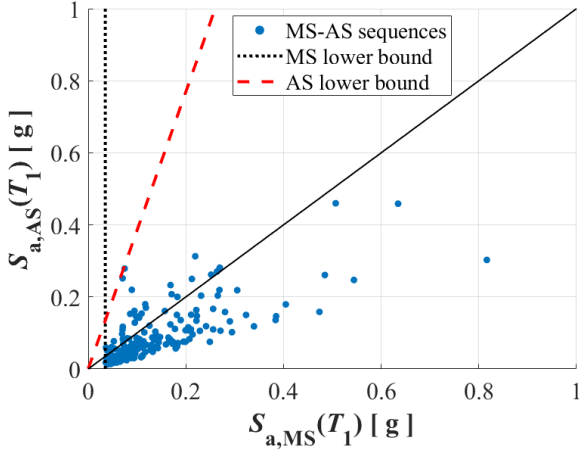


Figure 6: Distribution of the subset of 199 MS-AS records (extracted from Goda & Taylor 2012).

#### 5. PERFORMANCE-BASED ASSESSMENT

Fragility curves of the undamaged structure are derived by performing a Cloud Analysis employing only the MS of the sequences previously selected. The spectral acceleration corresponding to the fundamental period of the structure is used as intensity measure (IM). Two different engineering demand parameters (EDPs) are considered, namely the maximum ductility ( $\mu$ ) and cumulative ductility ( $\mu_c$ ) among all BRBs. Fragility curves are defined through probabilistic seismic demand models (PSDM, Cornell et al. 2002). The EDP-IM relationship is approximated by a power-law model and the demand is then assumed as lognormally distributed. Capacity

limits are set equal to 25 and 400 for  $\mu$  and  $\mu_c$  respectively (Fahnestock et al. 2003, Zona et al. 2012b). System fragility curves are obtained selecting for each record the maximum value of  $\mu$  and  $\mu_c$  demand among all the devices.

The effect of the cumulative damage is investigated by two different approaches, as shown in Figure 7, based on sequential Cloud Analyses, as proposed by Jalayer & Ebrahimian (2017). The **Approach 1** focuses on the effect of damage accumulation and relies on artificial MS-AS sequences. Four MSs with increasing intensities, named  $MS^*_j$  with  $j=1, \dots, 4$ , are selected to represent different levels of initial damage. Subsequently, each  $MS^*_j$  is combined with the full set of 199 MS to derive artificial MS-AS sequences. The **Approach 2** allows to evaluate the potential of the AS to induce additional damage, by using the real MS-AS sequences selected in Section 4.

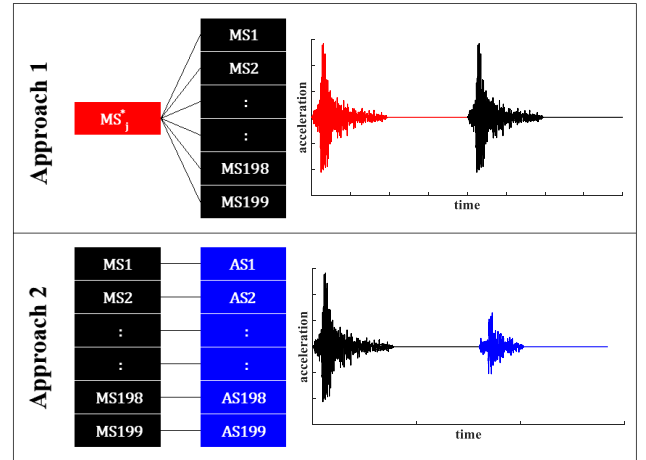


Figure 7: Sequential Cloud Analysis Approaches.

It is noteworthy that a decay time of 40 s is used between MS and AS signals to ensure that free vibrations induced by the MS are fully damped before the AS is applied.

##### 5.1. Approach 1: Artificial sequences

Figure 8 shows the distribution of  $\mu$  and  $\mu_c$  demand values resulted from the Cloud Analysis of the undamaged structure. On the same Figure, the four selected  $MS^*_j$  events are identified. The latter are chosen to reproduce an initial level of

damage approximately equal to 20, 40, 60 and 80% of the capacity limits for both the EDPs.

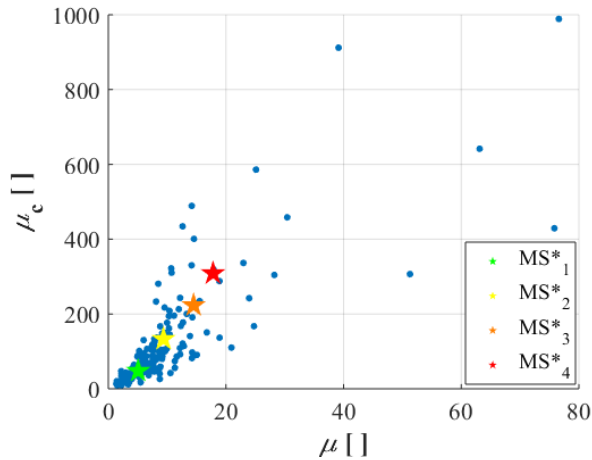


Figure 8: EDPs results from the Cloud Analysis of the undamaged structure and selected  $MS^*_j$  records.

Figure 9 shows the fragility curves conditioned to the four levels of damage considering  $\mu$  as EDP. The comparison with the fragility curve of the undamaged structure shows that, monitoring this EDP, the structural system is not affected by the imposed initial damage. This is due to the stable cyclic behavior of BRBs (as in Figure 4) and to the elastic behavior of the MRF.

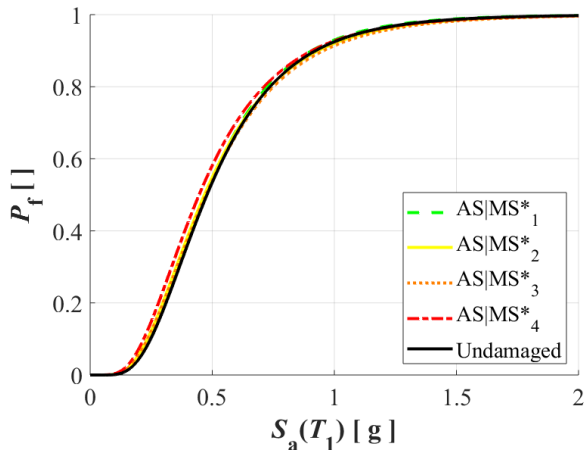


Figure 9:  $\mu$ -based AS fragility curves, conditioned to the level of damage induced by  $MS^*_j$ .

However, even if not captured by the comparison in Figure 9, it is noteworthy that the presence of AS can affect the local response of BRBs. In fact, when multiple events are considered, the ductility demand of the BRBs is accumulated at each event and could lead to the

failure of the device. Fragility curves conditioned to the four levels of damage considering  $\mu_c$  as EDP are plotted in Figure 10.

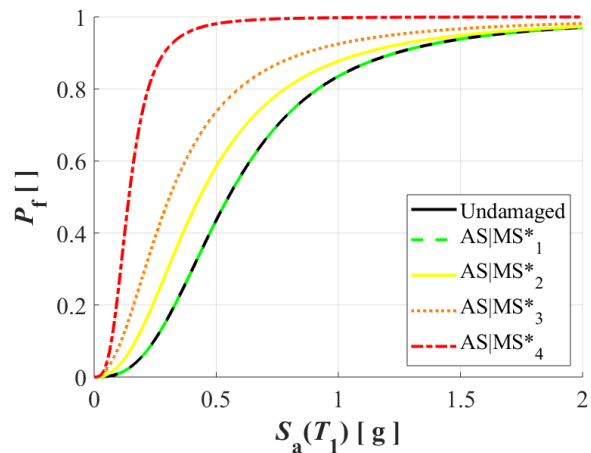


Figure 10:  $\mu_c$ -based AS fragility curves, conditioned to the level of damage induced by  $MS^*_j$ .

In this case, increasing levels of initial damage induced by the MS are associated with a higher probability of collapse. BRBs that sustained a MS with a small intensity are likely to sustain a following earthquake without a significant increase in the probability of failure. Viceversa, in presence of strong MS events, replacement of BRBs might be recommended

## 5.2. Approach 2: Real sequences

The potential failure of BRBs induced by the attainment of maximum cumulative ductility capacity has been observed above. However, Approach 1 neglects the statistical correlation that exists between MS and AS ground-motion properties. Differently, Approach 2 allows to evaluate the effect of cumulative damage induced by real MS-AS sequences. In this case, a traditional PSDM approach is not feasible because of the limited amount of strong sequences allowing the structure to exceed its collapse capacity. Hence, conditioned fragility curves cannot be derived.

Figure 11 shows the probability density function (*pdf*) for  $\mu_c$  for both the undamaged structure (MS events only) and the structure subjected to the full real MS-AS sequences. In particular, recorded values of  $\mu_c$  are fitted by an inverse Gaussian distribution to determine the

corresponding *pdf* where the Bayesian information criterion is used to determine the best fitting distribution, as done in Stillmaker et al. (2016).

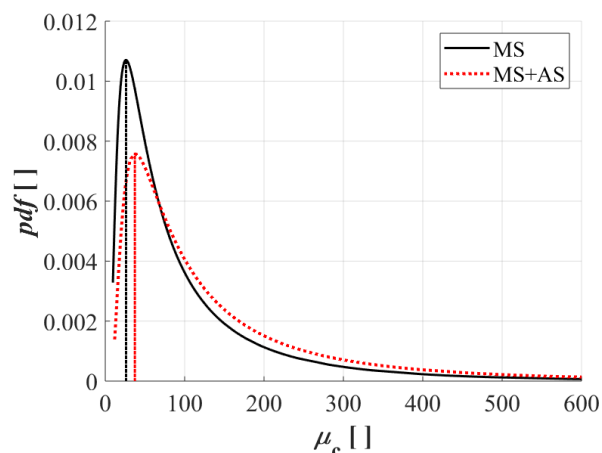


Figure 11: Pdf of  $\mu_c$  demand for the undamaged and damaged structure.

The two  $\mu_c$  demand curves show a negligible variation in the mean values between MS and full MS-AS sequences. Hence, even though the BRBs' capacity can be affected by multiple events (as seen in Approach 1), this preliminary result shows that real AS sequences are not expected to significantly increase the  $\mu_c$  demand.

## 6. CONCLUSIONS

The present paper has explored the behavior of steel dual systems comprising MRFs and BRBFs. The efficacy of a design procedure has been first investigated and the seismic behavior of a case-study building has then been assessed by means of Cloud Analysis accounting for MS-AS sequences. The results show that the combination of BRBFs and MRFs allows to design resilient structures able to successfully sustain MS-AS sequences. Two different sequential Cloud Analysis approaches have been proposed and tested for the index frame to assess the effect of cumulative damage induced by aftershocks. Even though a potential reduction in the BRBs' capacity is observed when referring to artificial MS-AS sequences, analyses performed using real sequences have shown that the  $\mu_c$  demand within BRBs is not significantly affected by the AS.

Future work is needed to support findings of this study. In particular, additional case studies with different design parameters will be evaluated; moreover, the effect of real sequences accounting for multiple AS will be investigated.

## ACKNOWLEDGEMENTS

The support of Prof. Katsuchihiro Goda that provided real MS-AS sequences, as well as the fruitful discussions on the detailed BRBs OpenSees modeling with Prof. Alessandro Zona and Prof. Quan Gu are gratefully acknowledged.

## REFERENCES

- ASCE/SEI 7-10. (2010). *Minimum design loads for buildings and other structures*. American Society of Civil Engineers, Reston, VA.
- Ariyaratana, C., Fahnestock, L.A. (2011). "Evaluation of buckling-restrained braced frame seismic performance considering reserve strength". *Eng. Str.*, 33(1), 77-89.
- Baiguera, M., Vasdravellis, G., Karavasilis, T.L. (2016). "Dual seismic-resistant steel frame with high post-yield stiffness energy-dissipative braces for residual drift reduction." *J. Constr. Steel Research*, 122, 198–212.
- Castro, J.M., Elghazouli, A.Y., Izzuddin, B.A. (2005). "Modelling of the panel zone in steel and composite moment frames", *Eng. Struct.*, 27(1), 129–144.
- Cornell, C.A., Jalayer, F., Hamburger, R.O., Foutch, D. A. (2002). "Probabilistic Basis for 2000 SAC Federal Emergency Management Agency Steel Moment Frame Guidelines", *J. Str. Eng.*, 128(4), 526-533.
- Dall'Asta, A., Ragni, L., Tubaldi, E., Freddi, F. (2009). "Design methods for existing r.c. frames equipped with elasto-plastic or viscoelastic dissipative braces", *ANIDIS, Italian Conf. on Earthq. Eng.*, Bologna, Italy.
- Di Sarno, L., Manfredi, G. (2010). "Seismic retrofitting with buckling restrained braces: Application to an existing non-ductile RC framed building", *Soil Dyn. & Earthq. Eng.*, 30(11), 1279–1297.
- European Committee for Standardization. (2004). "Eurocode 8: Design provisions for earthquake resistance of structures, Part 1.1: General rules seismic action and rules for buildings". Brussels.

- Faccioli, E., Paolucci, R., Rey, J. (2004). "Displacement Spectra for long period", *Earthq. Spectra*, 20(2), 347-376.
- Fahnestock, L.A., Sause, R. Ricles, J.M., Lu L.W. (2003). "Ductility demands on buckling-restrained braced frames under earthquake loading", *Earthq. Eng. & Eng. Vibr.*, 2(2), 255-268.
- Fajfar, P. (2000). "A Nonlinear Analysis Method for Performance Based Seismic Design", *Earthq. Spectra*, 16(3), 573-592.
- Freddi, F., Tubaldi, E., Ragni, L., Dall'Asta, A. (2013). "Probabilistic performance assessment of low-ductility reinforced concrete frame retrofitted with dissipative braces". *Earthq. Eng. & Str. Dyn.*, 42(7), 993-1011.
- Freddi, F., Dimopoulos, C., Karavasilis, T.L. (2017). "Rocking damage-free steel column base with friction devices: design procedure and numerical evaluation", *Earthq. Eng. & Str. Dyn.*, 46(14), 2281-2300.
- Garcia, R., Sullivan, T., Della Corte, G. (2010). "Development of a Displacement-Based Design Method for Steel Frame-RC Wall Buildings", *J. of Earthq. Eng.*, 14(2), 252-277.
- Goda, K., Taylor, A.C. (2012). "Effects of aftershocks on peak ductility demand due to strong ground motion records from shallow crustal earthquakes", *Earthq. Eng. & Str. Dyn.*, 41(15), 2311-2330.
- Gu, Q., Zona, A., Peng, Y., Dall'Asta, A. (2014). "Effect of buckling-restrained brace model parameters on seismic structural response", *J. of Constr. Steel Research*; 98,100-113.
- Ibarra, L.F., Medina, R.A., Krawinkler, H. (2005). "Hysteretic models that incorporate strength and stiffness deterioration", *Earthq. Eng. & Str. Dyn.*, 34(12), 1489-1511.
- Jalayer, F., Ebrahimian, H. (2017). "Seismic risk assessment considering cumulative damage due to aftershocks", *Earthq. Eng. & Str. Dyn.*, 46(3), 369-389.
- Kiggins, S., Uang, C.M. (2006). "Reducing residual drift of buckling-restrained braced frames as dual system", *Eng. Str.*, 28(11), 1525-1532.
- Lignos, D.G., Krawinkler, H. (2011). "Deterioration Modelling of Steel Components in Support of Collapse Prediction of Steel Moment Frames under Earthquake Loading", *J. Str. Eng.*, 137(11), 1291-1302.
- Maley, T.J., Sullivan, T.J., Della Corte, G. (2010). "Development of a Displacement-Based Design Method for Steel Dual Systems with Buckling-Restrained Braces and Moment-Resisting Frames", *J. Earthq. Eng.*, 14(S1), 106-140.
- McKenna, F., Fenves, G.L., Scott, M.H. (2006). OpenSees: open system for earthquake engineering simulation. *PEER Center*, Berkeley, California.
- Priestley, M.J.N., Calvi, G.M., Kowalski, M.J. (2007). *Displacement Based Seismic Design of Structures*. IUSS Press, Pavia, Italy.
- Ragni, L., Zona, A., Dall'Asta, A. (2011). "Analytical expressions for preliminary design of dissipative bracing systems in steel frames", *J. Constr. Steel Research*, 67(1), 102-113.
- Raghunandan, M., Liel, A.B., Luco, N. (2015). "Aftershock collapse vulnerability assessment of reinforced concrete frame structures", *Earthq. Eng. & Str. Dyn.*, 44(3), 419-439.
- Sabelli, R., Mahin, S., Chang, C. (2003). "Seismic demands on steel braced frame buildings with buckling-restrained braces", *Eng. Str.*, 25(5), 655-666.
- Stillmaker, K., Kanvinde, A., Galasso, C. (2016). "Fracture mechanics-based design of column splices with partial joint penetration welds", *J. Str. Eng.*, 142(2), 04015115.
- Terán-Gilmore, A., Ruiz-García, J., Bojórquez-Mora, E. (2015). "Flexible Frames as Self-Centering Mechanism for Buildings Having Buckling-Restrained Braces", *J. Earthq. Eng.*, 19(6), 978-990.
- Tubaldi, E., Freddi, F., Zona, A., Dall'Asta, A. (2017) "Seismic Performance of Steel Dual Systems with BRBs and Moment-Resisting Frames", 16<sup>th</sup> ECEE, *European Conf. Earthq. Eng.*, Thessaloniki, Greece.
- Zareian, F., Medina, R.A. (2010). "A practical method for proper modelling of structural damping in inelastic plane structural systems", *Computer & Structures*, 88(1), 45-53.
- Zona, A., Dall'Asta, A. (2012a). "Elastoplastic model for steel buckling-restrained braces", *J. Constr. Steel Research*, 68(1), 118-125.
- Zona, A., Ragni, L., Dall'Asta, A. (2012b). "Sensitivity-based study of the influence of brace over-strength distributions on the seismic response of steel frame with BRBs", *Eng. Str.*, 37, 179-192. 24.